ARTICLE IN PRESS

Atmospheric Environment xxx (xxxx) xxx

Contents lists available at ScienceDirect

Atmospheric Environment

journal homepage: http://www.elsevier.com/locate/atmosenv

A comparative assessment of regional representativeness of EDGAR and ECLIPSE emission inventories for air quality studies in India

Abhishek Upadhyay[a,*], Sagnik Dey[a,b], Pramila Goyal[a,c]

[a] *Centre for Atmospheric Sciences, Indian Institute of Technology Delhi, New Delhi, India*
[b] *Centre of Excellence for Research on Clean Air, Indian Institute of Technology Delhi, New Delhi, India*
[c] *The Northcap University, Gurugram, India*

HIGHLIGHTS

- Anthropogenic $PM_{2.5}$ is simulated over India with EDGAR-HTAP and ECLIPSE emission Inventory.
- Anthropogenic $PM_{2.5}$ using ECLISPE is 26% higher than that using EDGAR inventory.
- BC:OC ratio simulated by both the inventories varies in the range 3–5.
- Pollution build-up is pushed towards eastern part of Gangetic basin in the winter season.
- Diurnal amplitude in anthropogenic $PM_{2.5}$ often exceeds 15 $\mu g/m^3$.

GRAPHICAL ABSTRACT

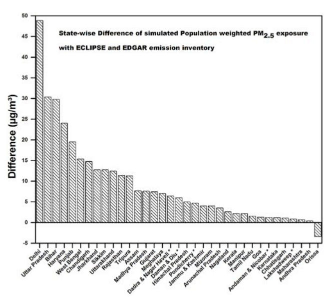

ARTICLE INFO

Keywords:
EDGAR-HTAP
ECLIPSE
WRF-Chem
$PM_{2.5}$
BC
OC
Emission inventory
Air quality
India

ABSTRACT

Ambient $PM_{2.5}$ (fine particulate matter) exposure is one of the leading health risk factors in India. The role of chemical transport models (CTMs) in air quality management is well recognized today. However, effectiveness of CTM outputs critically depends on accuracy of emission inventory. Here we evaluate anthropogenic $PM_{2.5}$ simulated by WRF-Chem using two major inventories - EDGAR and ECLIPSE with satellite and MERRA-2 reanalysis data. We found that both inventories show similar accuracy statistically (correlation coefficients, R of 0.87 and 0.9 and RMSEs of 8.4 and 10.2 $\mu g/m^3$ for EDGAR and ECLIPSE, respectively) at national scale, but with significant regional variation. The simulated anthropogenic populated $PM_{2.5}$ exposure is high with ECLIPSE emission compare to EDGAR for most of the states. In some populated states Delhi, Uttar Pradesh, Haryana, Bihar, Uttarakhand, Rajasthan, Punjab and few less populated states Sikkim, Tripura exposure is exceeding more than 30% with ECLIPSE emission inventory compare to EDGAR. After the monsoon is withdrawn, pollution builds up in the western Indo-Gangetic Basin (IGB), while it is pushed towards eastern IGB in the winter season. Diurnal amplitude in anthropogenic $PM_{2.5}$ exceeds 15 $\mu g/m^3$ in large parts of India especially during the post-monsoon to winter season suggesting that exposure modeling needs to be carried out with higher temporal frequency for better health burden assessment.

* Corresponding author.
E-mail address: abhiupadhyay777@gmail.com (A. Upadhyay).

https://doi.org/10.1016/j.atmosenv.2019.117182
Received 24 June 2019; Received in revised form 7 October 2019; Accepted 23 November 2019
Available online 30 November 2019

1. Introduction

Exposure to particulate matter with diameter less than 2.5 μm (referred to as $PM_{2.5}$) is the largest environmental health risk factor in India (Dandona et al., 2017). The Global Burden of Disease (GBD) study revealed that annual population weighted mean exposure to ambient $PM_{2.5}$ in India was 89.9 $\mu g/m^3$ (95% uncertainty interval [UI] 67.0–112.0 $\mu g/m^3$) in 2017 (Balakrishnan et al., 2019). This implies that 76.8% population was exposed to ambient $PM_{2.5}$ concentrations exceeding annual national ambient air quality standard (NAAQS). As a result, 670,000 (550,000–790,000) premature deaths and 0.9 (0.8–1.1) year life expectancy loss were attributed to ambient $PM_{2.5}$ exposure in India in 2017 (Balakrishnan et al., 2019). Several other studies in India provided evidence to link air pollution exposure to various health outcomes such as low birthweight (Balakrishnan et al., 2015), all-cause mortality (Balakrishnan et al., 2011; Dholakia et al., 2014; Rajarathnam et al., 2011), children lung function (Awasthi et al., 2010), respiratory morbidity (Kumar et al., 2007), and emergency hospital visits (Pande et al., 2002). The economic impact of air pollution in India was pegged at a massive USD 800 billion in 2016 (OECD, 2016).

Due to the staggering health burden attributed to air pollution, a study conducted by an expert committee formed by the Govt. of India (Sagar et al., 2016) has argued that the problem of air pollution needs to be treated from a health-centred perspective, for which the first step is to generate ambient $PM_{2.5}$ exposure statistics for the entire country with high accuracy. Unfortunately, the ground-based monitoring of $PM_{2.5}$ is not adequate in India as only 1 monitor operates per 6.8 million people (Martin et al., 2019) and the spatial distribution is also non-uniform across India (see www.cpcb.nic.in for the locations of continuous and manual monitoring). This leaves a large part of India including the entire rural area unmonitored. Satellite data have been utilized to fill this spatial sampling gap (e.g. Dey et al., 2012; Van Donkelaar et al., 2016), where scaling factors to convert satellite-retrieved aerosol optical depth (AOD) to $PM_{2.5}$ were generated by a chemical transport model (CTM) (van Donkelaar et al., 2010). However, satellites have temporal gap and therefore, complimentary information from CTMs are highly useful to fill the spatial and temporal gap in $PM_{2.5}$ monitoring.

Another critical component of air quality management is the information about relative contributions of various sources at regional scale. While the traditional methods of chemical analysis and receptor modelling can provide valuable information at city level, it is difficult to apply such methods at national scale. CTMs are also proven to be useful in source apportionment at a regional scale when a particular source is switched off in a simulation and the simulated $PM_{2.5}$ without that source in comparison to simulated $PM_{2.5}$ with all the sources can be attributed to the relative contribution of that particular source. Using this 'subtraction method', several studies (Chafe et al., 2015; Conibear et al., 2018., Global Burden of, 2018; Upadhyay et al., 2018a) have confirmed that household emissions contribute the largest share to ambient $PM_{2.5}$ in India. While these studies agree broadly in terms of relative contributions of individual sources, the magnitudes vary (Chowdhury et al., 2019a) due to (a) incorporation of different emission inventory, (b) differences in model simulated meteorology that in turn depends on the initial and boundary conditions, and (c) model physics. Systematic approach is required to understand the influences of these three factors in model-simulated $PM_{2.5}$. Inter-comparison of various CTMs using the same emission inventory and meteorology (Rao et al., 2010) would advance understanding of the nuances of the parameterization schemes in the models. On the other hand, use of various inventories in a single model would help understanding the representativeness of the inventory. This is an important issue as India does not have any national emission inventory that is periodically updated. Several regional (Behera and Sharma, 2011; Guttikunda and Calori, 2013; Pandey et al., 2014; Sadavarte and Venkataraman, 2014; Sharma and Dixit, 2016) and global (Janssens-Maenhout et al., 2012; Stohl et al., 2015) emission inventories are available for use in air quality studies in India. It is difficult to assess the representativeness of these inventories in mimicking the real anthropogenic $PM_{2.5}$ distribution directly due to their methodological differences.

In this work, we simulate anthropogenic $PM_{2.5}$ over India by WRF-Chem using the two widely used global emission inventories – EDGAR-HTAP (Emission Database for Global Atmospheric Research – Hemispheric Transport of Air Pollution) and ECLIPSE (Evaluating the Climate and Air Quality Impact of Short-Lived Pollutants). WRF-Chem is chosen as the CTM as it is a community model and previously has been used by various researchers to examine aerosol distribution over India (Bran and Srivastava, 2017; Conibear et al., 2018; Upadhyay et al., 2018a). We then evaluate the simulated anthropogenic $PM_{2.5}$ with satellite observations and intercompare the concentrations of primary and secondary pollutants from the two inventories in view of atmospheric processes and sources. The present work provides a framework to evaluate the representativeness of these inventories in the Indian context for studying air quality and its space-time variation.

2. Methodology

2.1. Model setup

Online coupled WRF-Chem is a combination of Weather Research Forecasting (WRF) and chemistry model, this is developed and maintained at National Centre for Atmospheric Research (NCAR) for simulating meteorological parameters and chemical composition of atmosphere simultaneously (Fast et al., 2006; Grell et al., 2005). Simulation has been performed with WRF-Chem 3.6 at a 10 km × 10 km resolution over the domain that centres around 28.6 N, 77.2 E and covers all the land area of India (Fig. 1). The domain has horizontally 345 × 345 grid points and 30 vertical levels with the top set at 50 hPa. Physics and chemistry schemes used in model setup for this study are summarized in Table 1. Meteorological initial and boundary conditions have been generated using NCEP – FNL (National Centre for Environment Protection - Final Analysis) data that includes all required meteorological fields at a spatial resolution of 1° × 1° for every 6 h. 24 category land-use data from United States Geographical Survey (USGS) has been used in this study.

Two sets of WRF-Chem simulations have been performed for the entire year 2010 using EDGAR-HTAP and ECLIPSE. Separate simulation for each month has been performed and these monthly simulations have been averaged to get results at annual scale. First 24-h data from each month has been left as spin-up. Anthropogenic $PM_{2.5}$ has been obtained by removing simulated natural $PM_{2.5}$ from total simulated $PM_{2.5}$.

2.2. Emission inventory

We use EDGAR-HTAP and ECLIPSE emission inventories for the simulations. EDGAR project is managed by Joint Research Centre (JRC) of European Commission. Version 2 of EDGAR-HTAP has been developed for SO_2, NO_x, CO, NMVOC, NH_3, PM_{10}, $PM_{2.5}$, BC and OC atresolution of 1° × 1° for the year 2008 and 2010 (https://edgar.jrc.ec.europa.eu/htap_v2/). This emission inventory has been developed by compiling regional gridded emission inventories developed in various part of world. Emission inventory developed under project Model-Inter Comparison Study has been used for Asian countries like China and India (Janssens-Maenhout et al., 2015; Li et al., 2017), whereas emission inventories from United States Environmental Protection Agency (USEPA), Environment Canada, European Monitoring and Evaluation Programme has been used for USA, Canada and Europe respectively. EDGAR-HTAP has considered all major emission sectors like residential, transportation, industry and energy sector. Each of these sectors consists of emissions from different activities included under the sector. For example, the residential sector includes residential cooking, heating, lightening, solid waste treatment, whereas transport sector includes

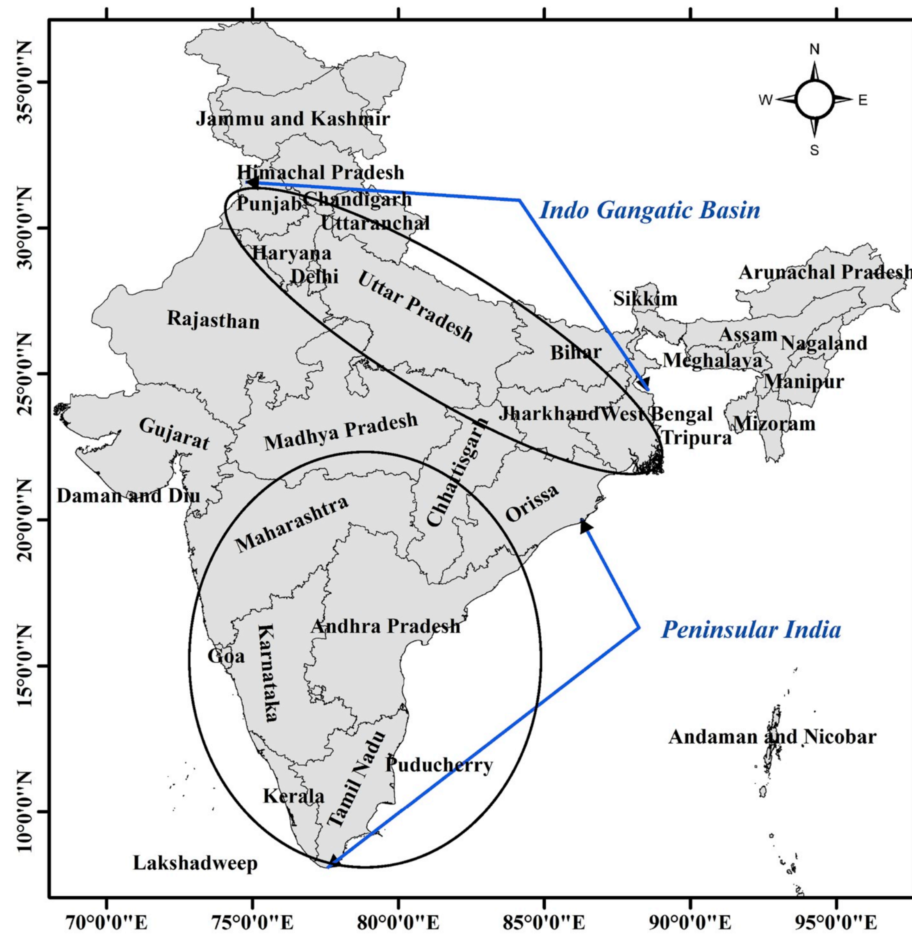

Fig. 1. Model domain with boundaries of states and the union territory (UT) of India. Indo-Gangatic Basin and Peninsular India are demarcated.

emissions from road, railway, inland water way and other ground transport of mobile machinery. Energy sector includes emissions from power generation units based on coal and industrial sector includes emissions from industrial processes, small and large scale combustion in industrial plant (Janssens-Maenhout et al., 2015).

ECLIPSE project of International Institute for Applied System Analysis (IIASA) aimed to generate gridded anthropogenic emissions inventory for the entire globe for different emission scenarios. Greenhouse gas – Air pollution Interactions and Synergies (GAINS) model has been used to estimate emissions using source characteristics and emission factor at a resolution of $0.5^{\circ} \times 0.5^{\circ}$ (Amann et al., 2011; Klimont et al., 2017; Stohl et al., 2015). In this work, we use year 2010 emission for species SO_2, NO_x, CO, VOC, NH_3, PM_{10}, $PM_{2.5}$, BC and OC (http://www.iiasa.ac.at/web/home/research/researchPrograms/air/ECLIPSEv5.html). Version 5 of ECLIPSE has been used in this study which has incorporated some previously unaccounted emission sources like flaring of associated petroleum gases (in oil and gas exploration sectors), kerosene lamp for lighting, diesel generator sets, high emitting vehicle, international shipping, refuse burning, and brick kiln. Emissions are grouped in 6 major anthropogenic sources - domestic, industrial, transportation, energy, agriculture, and waste treatment. Previously, Current legislation emission (CLE) and SLCP (Short-Lived Climate Pollutants) mitigation scenarios of ECLIPSE have been compared for future projections of anthropogenic $PM_{2.5}$ over India (Upadhyay et al., 2018b).

Spatial distributions of emissions of $PM_{2.5}$, BC, OC, SO_2 and NO_x from EDGAR and ECLIPSE for the year 2010 and their ratios over the Indian landmass are shown in Fig. 2. Since ECLIPSE inventory is at coarser resolution than that of EDGAR, ECLIPSE emission inventory has been redistributed to $0.1^{\circ} \times 0.1^{\circ}$ resolution from $0.5^{\circ} \times 0.5^{\circ}$ using the spatial gradient from EDGAR. The IGB (Indo-Gangetic Basin, that spans across north India and is bounded by Himalayan mountain in north and central Indian mountains in south, Fig. 1) and eastern India are local hotspots for BC and OC emission in India. BC and OC emissions are higher over parts of south-east and central India and lower over the IGB (Fig. 2*f* and *i*) in EDGAR compared to ECLIPSE. Emission hotspots for SO_2 and NO_x are distributed across India in both the inventories. Broadly, SO_2 emission is higher in ECLIPSE in larger part of India (Fig. 2*j*, *k* and *l*) than in EDGAR with urban hotspots showing opposing trend. On the contrary, NO_x emission is higher at urban hotspots in EDGAR, but at regional scale in ECLIPSE (Fig. 2*m*, *n* and *o*). Such regional differences are reflected in the simulated anthropogenic $PM_{2.5}$ discussed in the next section.

Table 1
List of physics and chemistry schemes along with their references used in WRF-Chem setup for this work.

Physics and Dynamics Scheme		References
Microphysics	Lin	Lin et al. (1983)
Short wave Radiation	Dudhia	Dudhia (1989)
Long wave Radiation	RRTM	Mlawer et al. (1997)
Surface physics	Unified NOAH Land Surface Model	Tewari et al. (2004)
PBL scheme	YSU	Hong et al. (2006)
Cumulus	Grell-Fretias	Grell and Freitas (2014)
Chemistry options		
Gas phase Chemistry	RADM2	Stockwell et al. (1990)
Aerosol Chemistry	GOCART	Chin et al. (2002)

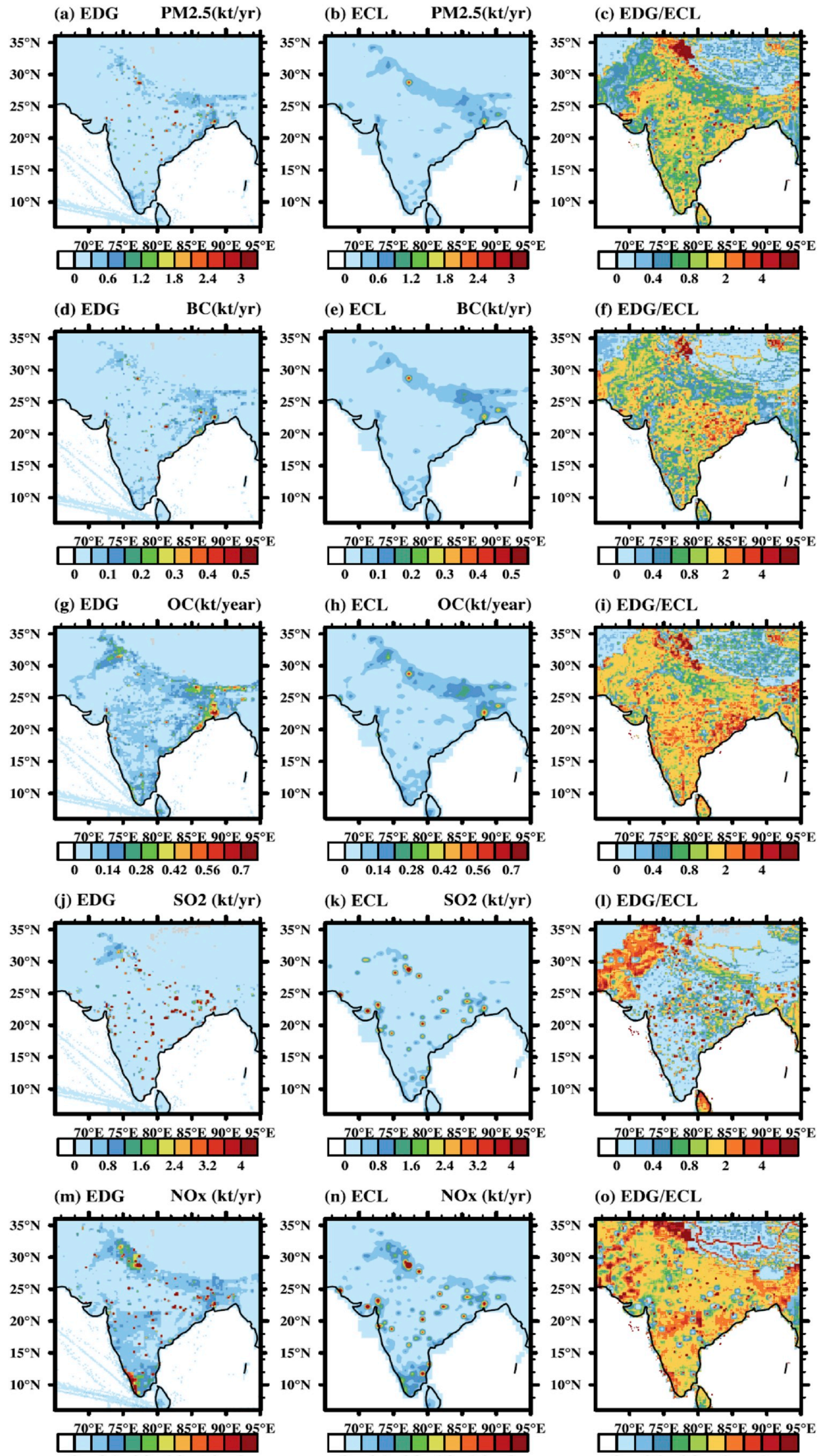

Fig. 2. EDGAR (left panel) and ECLIPSE (middle panel) emission for the year 2010, and their ratio (right panel) for (a, b and c) $PM_{2.5}$, (d, e and f) BC, (g, h and i) OC, (j, k and l) SO_2, and (m, n and o) NO_x.

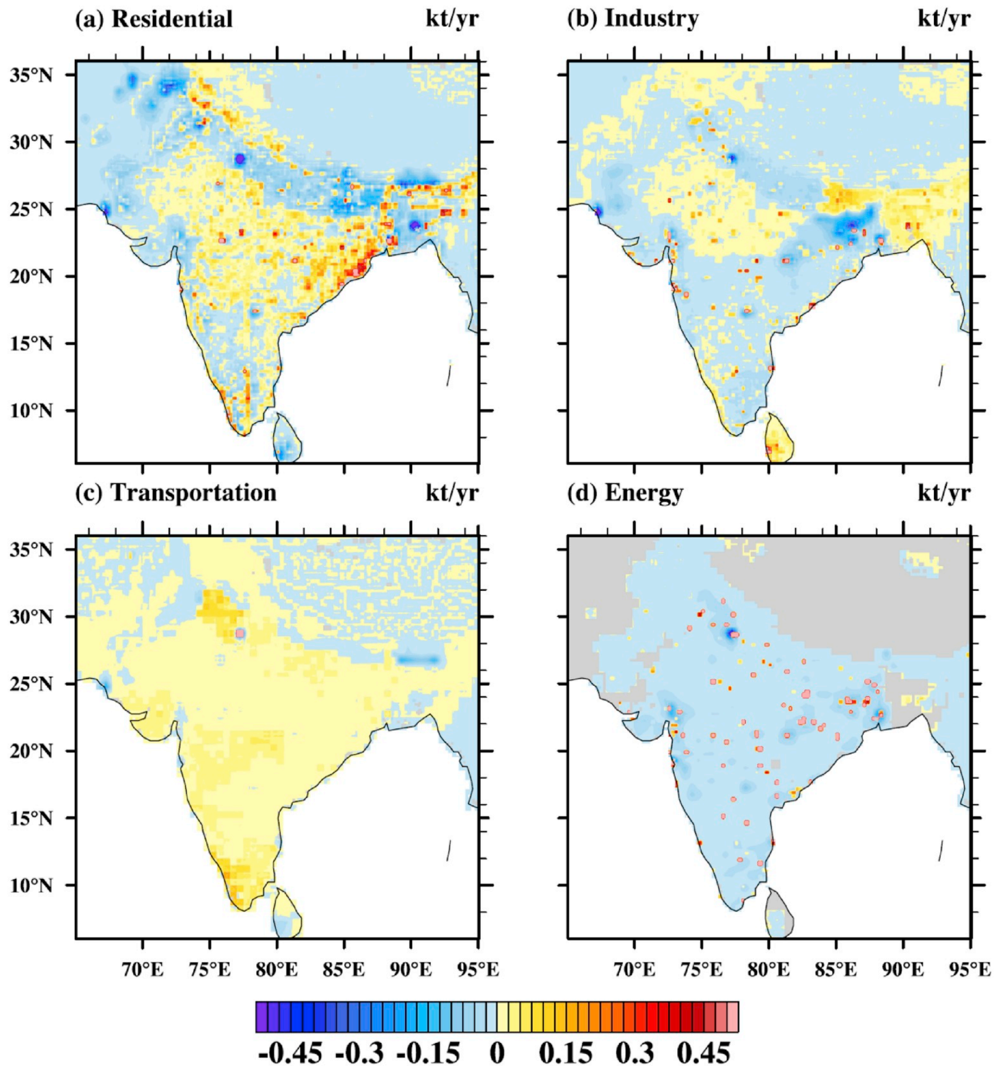

Fig. 3. Difference of $PM_{2.5}$ emissions between EDGAR and ECLIPSE from the (a) Residential, (b) Industrial, (c) Transport and (d) Energy sector.

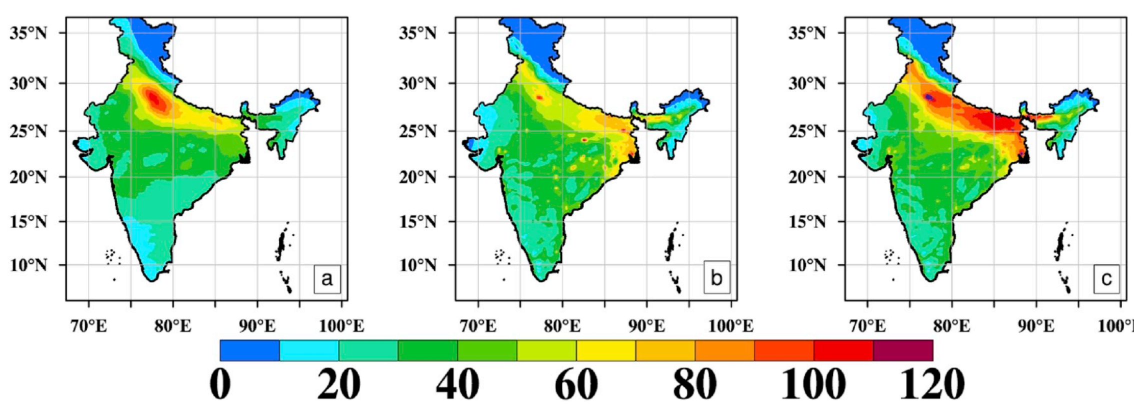

Fig. 4. (a) Satellite derived $PM_{2.5}$, and (b) simulated $PM_{2.5}$ using EDGAR and (c) using ECLIPSE. Unit is in μg m^{-3}.

Waste treatment emission is represented as a separate sector in ECLIPSE whereas in EDGAR-HTAP, it is included in residential sector. Total domestic emission from ECLIPSE (4708 kt/yr) is higher than EDGAR-HTAP (4559 kt/yr) over our study domain. Industrial emission in ECLIPSE (1506 kt/yr) is slightly higher than EDGAR-HTAP (1439 kt/yr) whereas emission from the transportation sector in EDGAR-HTAP (935 kt/yr) is two times higher than that in ECLIPSE (415 kt/yr). In ECLIPSE, agriculture waste burning emission has the smallest contribution (73 kt/yr) compared to other sectors but it is not included in EDGAR_HTAP emission. Differences in the spatial distribution of $PM_{2.5}$ between EDGAR and ECLIPSE for different emission sectors are shown in Fig. 3. It is revealed that in most of the IGB, ECLIPSE emission is higher than EDGAR and EDGAR emission is higher than ECLIPSE in the central and east India. Almost similar pattern is observed for the industrial

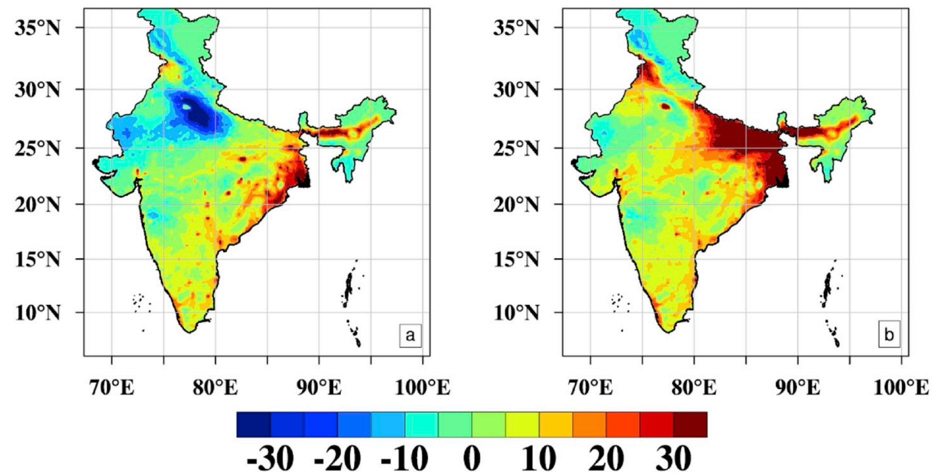

Fig. 5. Difference between CTM simulated and satellite-derived anthropogenic $PM_{2.5}$ using (a) EDGAR-HTAP and (b) ECLIPSE inventory.

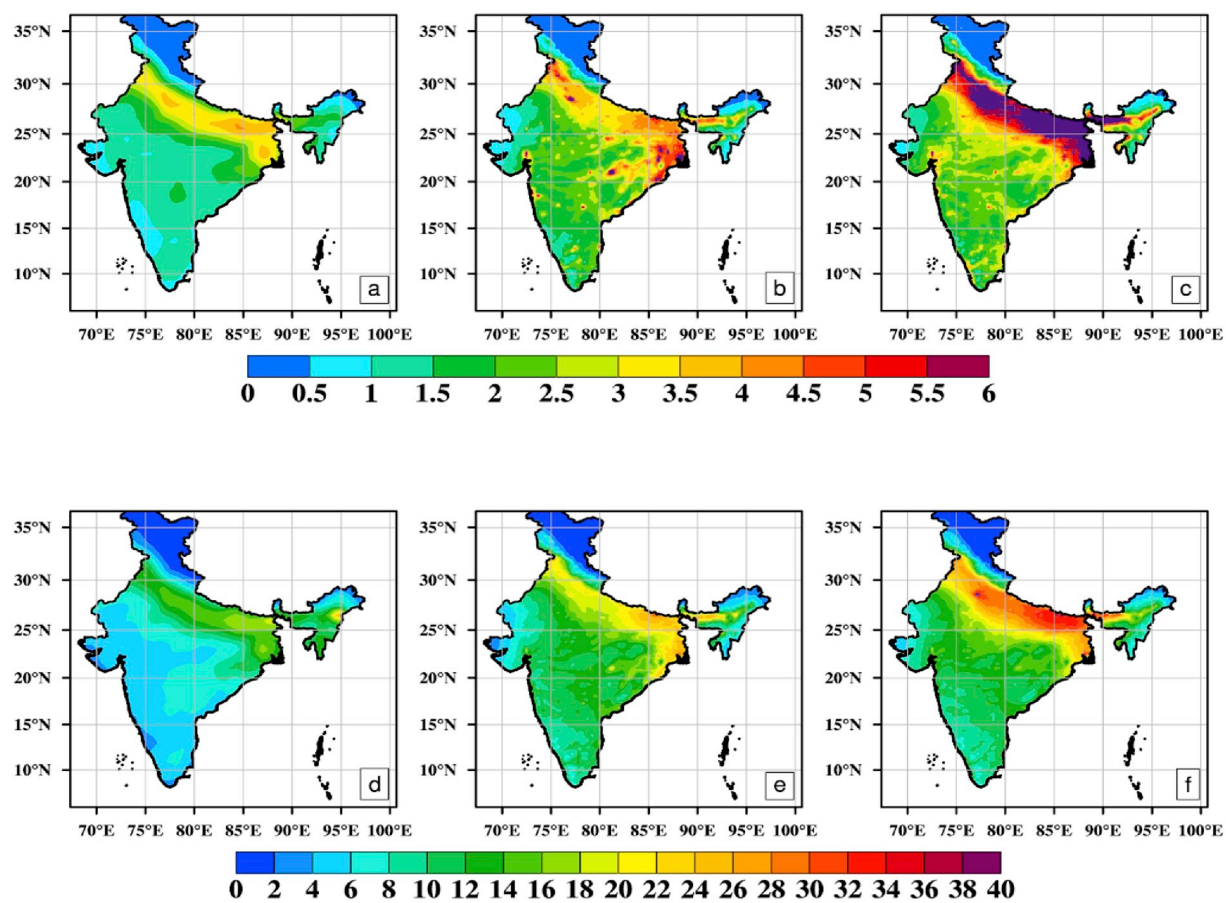

Fig. 6. BC (upper panel) and OC (lower panel) concentrations over India from (*a* and *d*) MERRA-2 (*b* and *e*) EDGAR-HTAP, and (*c* and *f*) ECLIPSE.

sector. Regional emission is higher in ECLIPSE for the industry and energy sectors, whereas EDGAR emissions are more restricted to local hotspots. In the transport sector, we observe the opposite picture.

2.3. Observational data for model evaluation

In 2010, ground-based $PM_{2.5}$ measurements were available only from 2 sites in Delhi and that too for few days, which are not adequate for robust comparison. The simulations could have been carried out for later years (*e.g.* after 2015) when ground-based $PM_{2.5}$ data are available from multiple sites across India; however, that would have led to large underestimation in emissions as anthropogenic emissions have been increasing in India (GBD Maps working group, 2018). Since our objective is to understand the regional representativeness of the inventory at national scale, we resort to satellite derived anthropogenic $PM_{2.5}$ database that has been generated at $0.1^{\circ}\times0.1^{\circ}$ resolution for the same year 2010 (Van Donkelaar et al., 2016). This $PM_{2.5}$ datasets has been generated using columnar aerosol optical depth (AOD) from multiple satellite products (MISR, MODIS Dark Target, MODIS Deep Blue, and SeaWiFS Deep blue), AERONET and a global chemical transport model

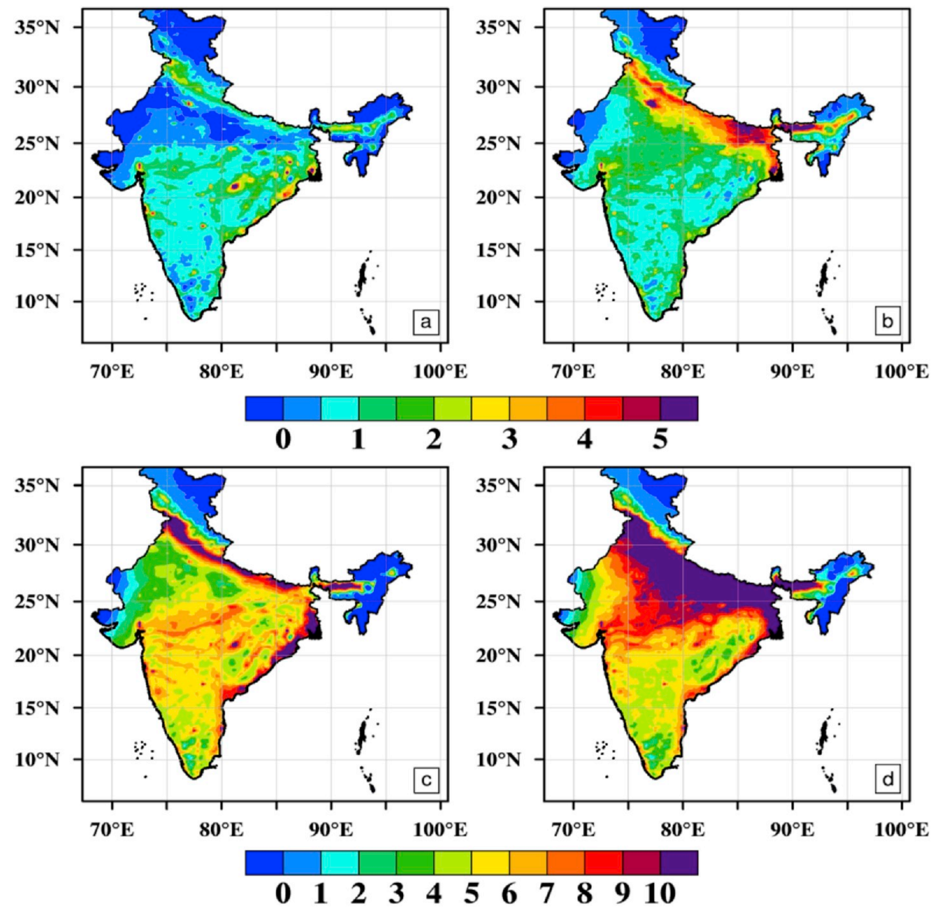

Fig. 7. Difference of simulated BC from (a) EDGAR and (b) ECLIPSE with MERRA-BC between (upper panel) and simulated OC from (c) EDGAR and (d) ECLIPSE with MERRA-OC (lower panel). Unit is in $\mu g/m^3$.

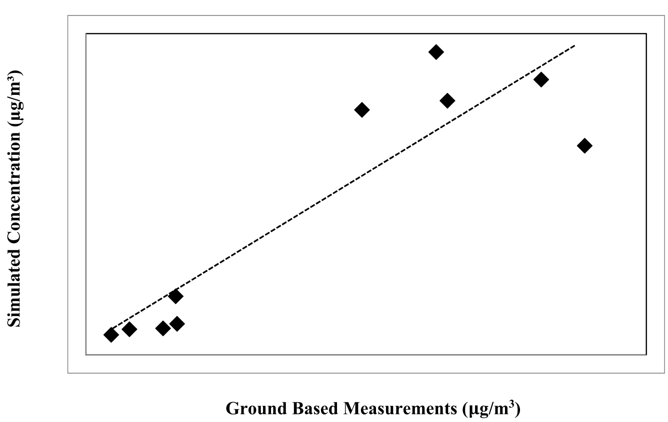

Fig. 8. Comparison between model-simulated BC (values lower than 10 $\mu g/m^3$) and OC (values higher than 15 $\mu g/m^3$) and ground-based measurements. In-situ observations are compiled from the literature (Pachauri et al., 2013; Ram et al., 2010; Ali et al., 2016; Kompalli et al., 2014; Joshi et al., 2016). The dotted solid line is 1:1 line.

GEOS-Chem simulations. Satellite retrieved and simulated AOD have been evaluated with AERONET to generate global continuous AOD field. The existing geophysical relation between AOD and $PM_{2.5}$ that varies spatially and temporally (at daily scale) obtained through simulations has been used to estimate surface $PM_{2.5}$ concentrations. This has been further calibrated with ground monitors by Geographically Weighted Regression method. Natural components (dust and sea-salt) are removed to estimate anthropogenic $PM_{2.5}$. More details of this database are available in Van Donkelaar et al. (2016).

Table 2
(First value) Pearson correlation coefficient (statistically significant at 99% CI) and (second value) Root Mean Square Difference (in $\mu g/m^3$) between simulated OC, BC and anthropogenic $PM_{2.5}$ with MERRA-2 OC, BC, and satellite derived anthropogenic $PM_{2.5}$.

	OC	BC	$PM_{2.5}$
EDGAR vs. ECLIPSE	0.97	0.93	0.97
	1.85	0.67	7.91
EDGAR vs. MERRA-2*/Satellite#	0.75*	0.86*	0.87#
	3.16*	0.47*	8.4#
ECLIPSE vs. MERRA-2*/Satellite#	0.78*	0.91*	0.90#
	3.89*	0.74*	10.2#

* MERRA data for BC and OC,
# Satellite data for $PM_{2.5}$

For BC and OC, we consider Modern-Era Retrospective analysis for Research and Application, Version 2 (MERRA-2) dataset in absence of adequate ground-based measurements. MERRA-2, a project of Global Modeling and Assimilation Office is first such kind of long term global reanalysis which assimilate space based observation of aerosol and includes interaction of aerosols with other physical processes in the climate system (Modeling et al., 2017). The MERRA-2 is based on advanced Goddard Earth Observing System (GEOS) model and Grid point statistical Interpolation (GSI) assimilation system. It provides surface mass concentration of BC and OC at 0.5° × 0.5° spatial resolution and hourly data of this product is available since 1980 at GES DISC. Since there are no suitable observations for the inorganic species in India

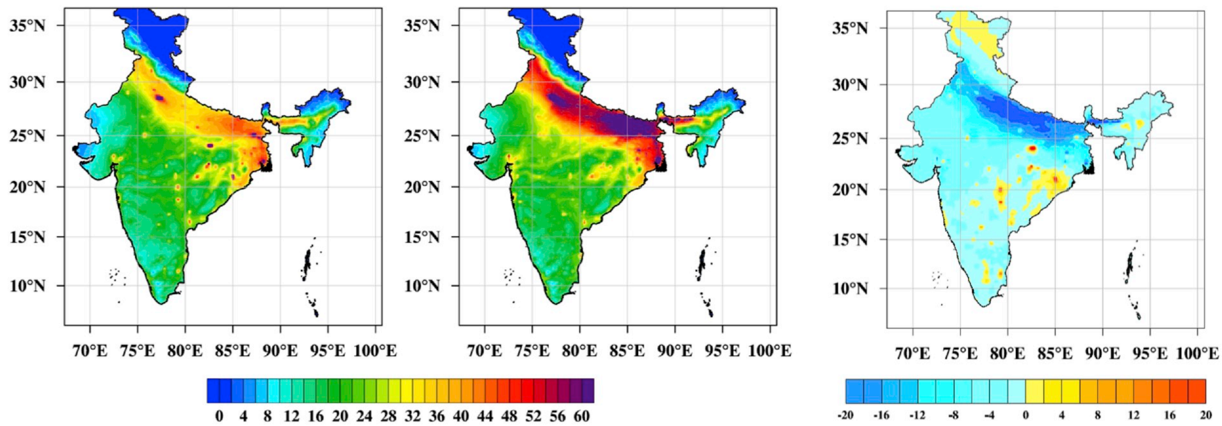

Fig. 9. Simulated other inorganic aerosols (OIA) using EDGAR-HTAP (left) ECLIPSE (middle) emission inventory, and their difference (right).

Table 3
Population-weighted mean ($\pm 1\sigma$) annual ambient anthropogenic $PM_{2.5}$ exposure (in $\mu g/m^3$) for 2010 simulated by WRF-Chem for each state and UTs (denoted by *) by EDGAR and ECLIPSE inventory and their difference.

	EDGAR	ECLIPSE
Andaman & Nicobar Islands*	4.0 ± 0.8	5.3 ± 1.0
Andhra Pradesh	35.0 ± 3.8	35.4 ± 3.4
Arunachal Pradesh	12.9 ± 4.4	16.4 ± 5.2
Assam	46.7 ± 7.0	54.4 ± 7.5
Bihar	70.3 ± 2.6	100.1 ± 3.2
Chandigarh	49.8 ± 00	64.6 ± 00
Chhatisgarh	40.8 ± 6.8	41.9 ± 5.2
Dadra & Nagar Haveli *	28.8 ± 1.3	35.3 ± 1.6
Daman & Diu *	32.7 ± 00	38.7 ± 00
Delhi*	73.7 ± 3.6	122.5 ± 8.1
Goa	25.1 ± 0.8	26.4 ± 0.9
Gujarat	29.6 ± 3.7	37.0 ± 4.3
Haryana	55.9 ± 4.0	79.9 ± 5.5
Himachal Pradesh	23.8 ± 7.7	28.7 ± 9.5
Jammu & Kashmir	20.0 ± 5.5	24.0 ± 6.1
Jharkhand	56.3 ± 4.5	69.0 ± 5.2
Karnataka	27.2 ± 2.0	28.4 ± 1.7
Kerala	28.9 ± 4.0	31.0 ± 4.2
Lakshadweep *	14.8 ± 1.5	15.6 ± 1.5
Madhya Pradesh	37.4 ± 2.2	45.0 ± 2.5
Maharashtra	38.7 ± 4.6	39.4 ± 4.9
Manipur	22.1 ± 2.7	24.2 ± 2.6
Meghalaya	30.2 ± 4.0	37.2 ± 4.2
Mizoram	15.3 ± 1.6	19.3 ± 1.8
Nagaland	23.6 ± 3.8	26.2 ± 3.8
Odisha	50.1 ± 5.3	46.7 ± 3.4
Pondicherry *	30.0 ± 1.0	34.7 ± 1.3
Punjab	58.1 ± 3.5	77.6 ± 4.2
Rajasthan	33.7 ± 2.7	45.1 ± 3.7
Sikkim	22.9 ± 6.5	35.7 ± 9.5
Tamil Nadu	30.7 ± 3.3	32.3 ± 3.3
Tripura	33.9 ± 4.4	45.1 ± 6.1
Uttar Pradesh	59.0 ± 2.2	89.4 ± 3.5
Uttarakhand	32.3 ± 6.4	44.8 ± 9.1
West Bengal	69.9 ± 6.4	85.2 ± 7.8
India	45.7 ± 3.7	57.6 ± 4.3

against which simulations can be compared, we have only inter-compared the simulated concentrations using the two different inventories.

3. Results

We first present the spatial distributions of anthropogenic $PM_{2.5}$ at annual scale over India from the two emission inventories and their comparisons with satellite-derived estimates. Then we compare simulations of carbonaceous aerosols (BC and OC) by the model with MERRA-2 data followed by inter-comparison of inorganic species simulated with these two inventories. Finally, we discuss the seasonal distribution of anthropogenic $PM_{2.5}$ over India and its diurnal pattern in the context of air quality assessment.

3.1. Evaluation of simulated anthropogenic $PM_{2.5}$ and carbonaceous aerosols

Anthropogenic $PM_{2.5}$ is estimated by subtracting natural component of $PM_{2.5}$ (dust and sea-salt) from the simulated total $PM_{2.5}$. Same model setup is used in both set of simulations, so it is assumed that equal amount of natural aerosols will be produced in both. Analysis of satellite-derived anthropogenic $PM_{2.5}$ reveals high annual concentrations over the IGB region and comparatively low concentrations over the Peninsular India. This north-south gradient is captured by both the inventories (Fig. 4) and also previously reported in other modelling as well as observational studies (e.g. Bran and Srivastava, 2017; Dey et al., 2012; Upadhyay et al., 2018a). However, even if the latitudinal gradient is broadly similar in satellite and model simulations, several key differences can be noted. A west (>100 μg m^{-3}) to east (60–100 μg m^{-3}) gradient in satellite-based $PM_{2.5}$ distribution in the IGB is somewhat captured in EDGAR simulation, though the spatial extent of the local hotspot around Delhi national capital region (NCR) is smaller in EDGAR than in the satellite observations. On the contrary, ECLIPSE simulation shows high $PM_{2.5}$ (>70 μg m^{-3}) over the entire IGB region without any noticeable longitudinal gradient. The spatial distributions of anthropogenic $PM_{2.5}$ over the Peninsular and central India are very similar in EDGAR and ECLISPE simulations. The biases in model simulated $PM_{2.5}$ (Fig. 5) relative to the satellite observations reveal that EDGAR under-estimates anthropogenic $PM_{2.5}$ over Delhi NCR by at least 20–30 μg m^{-3} and over the western arid regions by 10–20 μg m^{-3} while the bias in ECLISPE simulated $PM_{2.5}$ over Delhi NCR is positive. ECLIPSE over-estimates anthropogenic $PM_{2.5}$ by > 20 μg m^{-3} in the central and eastern IGB and Punjab, which may be attributed to larger emission of primary $PM_{2.5}$ and carbonaceous aerosols than in EDGAR (Fig. 2).

Residential $PM_{2.5}$ emission is higher across the IGB in ECLIPSE relative to EDGAR (Fig. 3). As the residential sector is the biggest contributor to ambient $PM_{2.5}$ in the central to eastern IGB (Upadhyay et al., 2018a; Chowdhury et al., 2019b), this is reflected in the simulations. ECLIPSE bias is slightly higher than EDGAR bias in the central India. Amazingly, both the emission inventories show similar biases in the rest of the country. Another notable observation is higher anthropogenic $PM_{2.5}$ in both the inventories at the urban hotspots in the Peninsular India (Fig. 5).

Not only anthropogenic $PM_{2.5}$, spatial distributions of BC and OC using both inventories match quite well with MERRA-2 BC and OC (Fig. 6). For example, OC (>15 $\mu g/m^3$) and BC (>3 $\mu g/m^3$) are very high

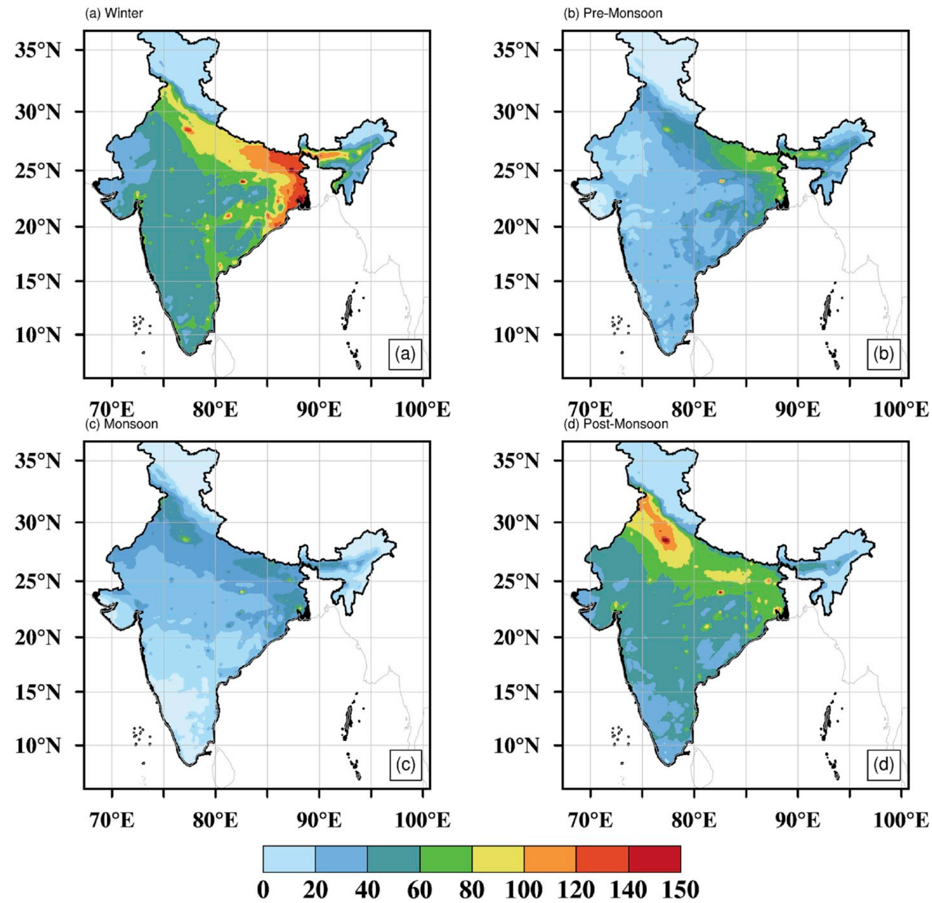

Fig. 10. Mean anthropogenic $PM_{2.5}$ simulated by WRF-Chem over India with EDGAR-HTAP emission in the (a) winter (Dec–Feb), (b) pre-monsoon (Mar–May), (c) monsoon (Jun–Sep) and (d) post-monsoon (Oct–Nov) seasons.

over the entire IGB region and gradually decrease towards south. OC is 3–5 times higher than BC in India. However, the BC hotspots over Delhi NCR and eastern India as seen in MERRA-2 are more pronounced in the EDGAR inventory. In fact, in EDGAR inventory several urban hotspots (*e.g.* Ahmedabad, Mumbai, Hyderabad, Bangalore, Kolkata, Bhubaneswar, Chennai) and hotspots around the coal belts in eastern India pop out which can be visible in the difference plot (Fig. 7). BC concentration is too high relative to MERRA-2 in the case of ECLIPSE inventory. Since meteorology is similar in the simulations with EDGAR and ECLIPSE, the difference (1–3 $\mu g/m^3$) can be attributed to only emission. Same inference can be drawn for OC where simulation with ECLIPSE inventory is 5–10 $\mu g/m^3$ higher in the IGB compared to EDGAR and is almost double than MERRA-2 OC. Unlike EDGAR, local hotspots are not prominent in ECLIPSE; rather it points towards a regional hotspot. Compared to BC, the bias in OC is higher in case of both ECLIPSE and EDGAR (Fig. 7). Since MERRA-2 is not direct measurement, it is difficult to attribute these biases solely to the emission inventories without evaluating the MERRA-2 reanalysis data with actual observations.

Very few direct measurements exist for the year 2010 for comparison, yet we pick up these values from the published literature to get a sense about the fidelity of the model simulations. We note that each point in Fig. 8 is either BC and OC measurements reported in the literature at various time scales (monthly, seasonal or averaged over several months). Though the points are few (hence statistics such as correlation is not shown), it can be interpreted that simulation of BC (as points lie closer to 1:1 line) is better than that of OC. In terms of statistics (Table 2), correlations between the two emission inventories in simulating BC, OC and $PM_{2.5}$ are reasonably strong ($R > 0.9$), and root mean square difference (RMSD) is also low compare to their average values. Strong correlation ($R > 0.85$) can also be seen for simulated $PM_{2.5}$ and BC compare to satellite derived and MERRA data. Simulated OC is also showing good correlation ($R > 0.75$) but comparatively less than BC and $PM_{2.5}$. RMSD is also supporting these statistics and all the values are statistically significant (at 99% CI).

Apart from BC and OC, secondary inorganic aerosol species constitute a major fraction of anthropogenic $PM_{2.5}$ and are collectively referred to as other inorganic aerosols (OIA) in the subsequent discussion. ECLIPSE OIA is higher than that from EDGAR in most parts of India (Fig. 9) except some positive patches in the central and eastern India. The difference in OIA remains mostly between ± 4 $\mu g/m^3$ suggesting similarity in the inventories in most parts of India except in the IGB and several local hotspots in and around central and east India. Larger OIA in ECLIPSE is observed relative to EDGAR in the IGB while the opposite trend is observed in the central and east India. These precursor gases (SO_2 and NO_2) once emitted into the atmosphere get converted to secondary inorganic species depending on the meteorological conditions. As similar atmospheric conditions are considered in the simulations, the observed differences in OIA concentrations can be attributed to the differences in gaseous precursors (Fig. 2) in the respective inventories. Once a substantial observation-based database of OIA is generated for India in future, the emissions of the gaseous precursors in these (or any other) inventories can be better evaluated.

3.2. State-level statistics of annual $PM_{2.5}$ exposure, seasonal variation and its diurnal pattern

Using Indian census data of 2011, we estimate annual anthropogenic $PM_{2.5}$ exposure at the state-level for both the inventories (Table 3) as such data are used for air pollution epidemiology and management. At a

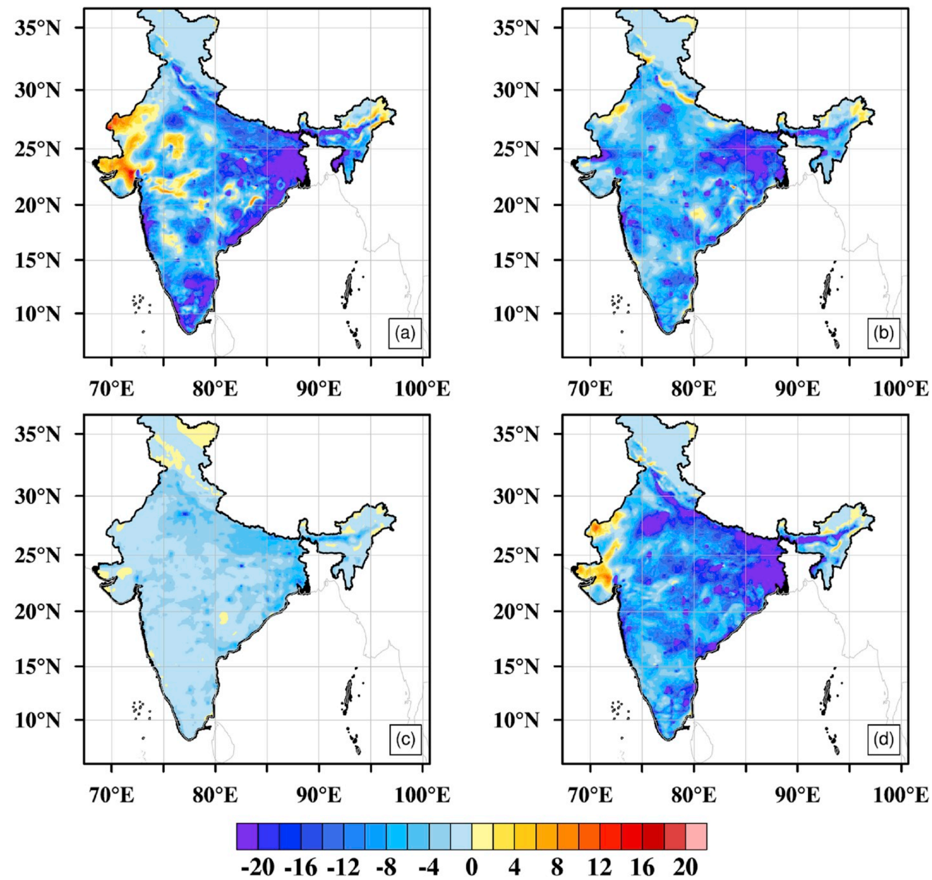

Fig. 11. Spatial distributions of difference between simulated anthropogenic $PM_{2.5}$ in day and night-time over India with EDGAR-HTAP emissions in the (a) winter (Dec–Feb), (b) pre-monsoon (Mar–May), (c) monsoon (Jun–Sep) and (d) post-monsoon (Oct–Nov) seasons.

national scale, simulated anthropogenic $PM_{2.5}$ in 2010 is estimated to be $45.7 \pm 3.7\ \mu g/m^3 g/m^3$ and $57.6 \pm 4.3\ \mu g/m^3$ with EDGAR and ECLIPSE emission inventory respectively. In general, simulated anthropogenic $PM_{2.5}$ exposure is higher for ECLIPSE inventory (relative to EDGAR) by >40% in populated states like Delhi, Uttar Pradesh, Haryana and Bihar, and by 30%–40% in Uttarakhand, Rajasthan and Punjab. In some lesser populated states in North-East India like Sikkim and Tripura, anthropogenic $PM_{2.5}$ exposure is 55% and 33% higher with ECLIPSE emission inventory compared to EDGAR. In the rest of the states, the exposure is little higher with ECLIPSE emission inventory in comparison with EDGAR, whereas for Odisha exposure is 6% higher with EDGAR compared to ECLIPSE. Since the same model and initial and boundary conditions are used in both the simulations, the observed difference can be only interpreted in terms of differences in emissions of primary and secondary pollutants.

The simulations also suggest that annual anthropogenic $PM_{2.5}$ exposure meets World Health Organization (WHO) air quality guideline ($10\ \mu g/m^3$) in only Andaman and Nicobar Island. In the states of Arunachal Pradesh and UTs (Union Territories) of Lakshadweep, it is lower than WHO interim target - 3 (IT-3, $15\ \mu g/m^3$). In Goa, Gujarat, Himachal Pradesh, Jammu and Kashmir, Manipur, Mizoram, Nagaland and Sikkim it lies between WHO IT-3 and IT-2 ($25\ \mu g/m^3$). In the remaining states and UTs, the exposure exceeds WHO IT-1 ($35\ \mu g/m^3$).

Seasonal (Fig. 10) and diurnal (Fig. 11) patterns in anthropogenic $PM_{2.5}$ exposure are discussed with simulations using EDGAR-HTAP emissions (as this is available at monthly temporal resolution and $0.1^\circ \times 0.1^\circ$ spatial resolution). Key features of the seasonal variation of $PM_{2.5}$ are as follows. In the winter (Dec–Feb) season, pollution is pushed back towards the eastern IGB by wind where it stagnates due to subsidence (Dey and Di Girolamo, 2011). High anthropogenic $PM_{2.5}$ over Delhi, Mumbai and several other hotspots are also visible. Rise in temperature and wind increases turbulence and diffusion and results in a decrease in anthropogenic $PM_{2.5}$ in the pre-monsoon (Mar–May) season across the country. While in most parts of the country $PM_{2.5}$ falls below $40\ \mu g/m^3$, it remains above $60\ \mu g/m^3$ in Delhi and eastern IGB. We note that natural dust also contributes to total $PM_{2.5}$ loading (that is not considered here) and an air pollution episode has been identified in Delhi region due to dust transport during this season (Chowdhury et al., 2019b). Precipitation during the monsoon season (Jun–Sep) results in wet deposition and the evidence of washout of pollution is visible as anthropogenic $PM_{2.5}$ decreases below $40\ \mu g/m^3$ even in the IGB. After the monsoon, wind speed reduces along with boundary layer making it stable and as a result, anthropogenic $PM_{2.5}$ starts building up in the post-monsoon (Oct–Nov) season. This post-monsoon build-up is most prominent in the Delhi NCR where it exceeds $150\ \mu g/m^3$ (Chowdhury et al., 2019b).

Another important aspect of air quality management is information about diurnal pattern of $PM_{2.5}$ exposure. Since the satellite-based estimates (Chowdhury and Dey, 2016; Dey et al., 2012) are representative of the morning and afternoon hours depending on the overpass time of the sun-synchronous satellites, $PM_{2.5}$ during night-time (or after the sunset) are not available for most parts of the country as the ground-based monitoring network is not adequate. Therefore, modeling exercise can fill this spatio-temporal data gap. Significant variation in meteorological parameters exist between day and night, especially temperature and planetary boundary layer height. These meteorological variations influence stability of the atmosphere which creates difference in day and night-time concentration of $PM_{2.5}$.

Fig. 11 shows mean seasonal difference between day (represented by concentration at 11:30 a.m. local time/06:00 UTC) and night-time (represented by concentration at 11:30 p.m. local time/18:00 UTC) $PM_{2.5}$ exposure in India as derived by WRF-Chem. Negative (positive) difference implies that night-time concentration is higher (lower) than daytime concentration. The least variation in diurnal amplitude is observed in the monsoon season whereas high (>15 μg/m^3) amplitude in eastern part of India is observed in the other seasons. In relative terms, highest percentage increase in night-time $PM_{2.5}$ is observed in the pre-monsoon season. Higher temperature in daytime results in high planetary boundary layer and better ventilation under unstable atmospheric condition. Such condition facilitates dispersion of pollutants during daytime. On the contrary, a reverse pattern is observed over the western arid region especially in the dry season. We think that calm night reduces $PM_{2.5}$ through settling of particles reversing the trend here, but this needs to be examined with in-situ measurements. In the monsoon season, $PM_{2.5}$ variability depends on the rainfall duration and intensity (Chowdhury et al., 2016). Also the diurnal variation of boundary layer is minimal and hence the diurnal amplitude of anthropogenic $PM_{2.5}$ is least in this season.

4. Summary and conclusions

In this work, we compare the two widely used emission inventory – EDGAR and ECLISE for their representativeness in examining anthropogenic $PM_{2.5}$ distribution and source apportionment in India. Since the model and meteorology used in the two simulations are exactly same, any difference in simulated anthropogenic $PM_{2.5}$ distribution can be attributed to the differences in the emissions of primary and secondary pollutants. We further examine the seasonal and diurnal pattern of anthropogenic $PM_{2.5}$ exposure. Key conclusions are as follows.

1. Spatial distributions of anthropogenic $PM_{2.5}$ as well as of carbonaceous aerosols (BC and OC) from WRF-Chem match reasonably well with satellite-derived and reanalysis products.
2 Anthropogenic $PM_{2.5}$ exposure from both the inventories are well correlated, but all-India population-weighted exposure using ECLIPSE is 26% higher than that using EDGAR.
3 Simulations using EDGAR demonstrate the local hotspots, while the pollution from ECLIPSE shows more of a regional picture, especially over a large part of the IGB.
4 Based on the statistics, none of the inventories can be considered better than the other uniformly across India. However spatial analysis of emissions and concentrations reveals that inventory at finer resolution can better represent the local hotspots. ECLIPSE inventory provides emission scenarios for the future and therefore is highly useful for policy analysis.
5 BC is better simulated than OC by both the inventories. Over India, OC concentration is observed to be 3-5 times of BC concentration.
6 The pollution oscillates within the IGB during the dry season. It builds up over the western IGB in the post-monsoon season and then pushed towards the central-to-eastern IGB in the winter season.
7 Large diurnal amplitude (often exceeding 15 g/m3) in PM2.5 in the dry season implies that satellite-derived exposure assessments would lead to underestimation in health burden estimates.

Declaration of competing interest

The authors declare that they have no known competing financial interests or personal relationships that could have appeared to influence the work reported in this paper.

Declaration of competing interest

The authors declare that they have no known competing financial interests or personal relationships that could have appeared to influence the work reported in this paper.

Acknowledgements

The first author acknowledges UGC fellowship. SD acknowledges Department of Science and Technology – Funds for Improvement of Science and Technology infrastructure in universities and higher educational institutions (DST-FIST) grant (SR/FST/ESII-016/2014) for computing support. We acknowledge NASA GMAO for providing MERRA-2 aerosol reanalysis data. All the simulation work has been performed at HPC at IIT Delhi. We thank the anonymous reviewers for providing valuable feedback to improve upon the earlier version of the manuscript.

Appendix A. Supplementary data

Supplementary data to this article can be found online at https://doi.org/10.1016/j.atmosenv.2019.117182.

References

Ali, K., Panicker, A.S., Beig, G., Srinivas, R., Acharja, P., 2015. Carbonaceous aerosols over pune and hyderabad (India) and influence of meteorological factors. J. Atmos. Chem. 73, 1–27. https://doi.org/10.1007/s10874-015-9314-4.

Amann, M., Bertok, I., Borken-kleefeld, J., Cofala, J., Heyes, C., Höglund-isaksson, L., Klimont, Z., Nguyen, B., Posch, M., Rafaj, P., Sandler, R., Schöpp, W., Wagner, F., Winiwarter, W., 2011. Environmental Modelling & Software Cost-effective control of air quality and greenhouse gases in Europe : modeling and policy applications. Environ. Model. Softw 26, 1489–1501. https://doi.org/10.1016/j.envsoft.2011.07.012.

Awasthi, A., Singh, N., Mittal, S., Gupta, P.K., Agarwal, R., 2010. Effects of agriculture crop residue burning on children and young on PFTs in North West India. Sci. Total Environ. 408, 4440–4445. https://doi.org/10.1016/j.scitotenv.2010.06.040.

Balakrishnan, K., Ramaswamy, P., Sambandam, S., Thangavel, G., Ghosh, S., Johnson, P., Mukhopadhyay, K., Venugopal, V., Thanasekaraan, V., 2011. Air pollution from household solid fuel combustion in India: an overview of exposure and health related information to inform health research priorities. Glob. Health Action 4, 5638. https://doi.org/10.3402/gha.v4i0.5638.

Balakrishnan, K., Sambandam, S., Ghosh, S., Mukhopadhyay, K., Vaswani, M., Arora, N. K., Jack, D., Pillarisetti, A., Bates, M.N., Smith, K.R., 2015. Household air pollution exposures of pregnant women receiving advanced combustion cookstoves in India: implications for intervention. Ann. Glob. Heal. 81, 375–385. https://doi.org/10.1016/j.aogh.2015.08.009.

Balakrishnan, K., Dey, S., Gupta, T., Dhaliwal, R.S., Brauer, M., Cohen, A.J., Stanaway, J. D., Beig, G., Joshi, T.K., Aggarwal, A.N., Sabde, Y., Sadhu, H., Frostad, J., Causey, K., Godwin, W., Shukla, D.K., Kumar, G.A., Varghese, C.M., Muraleedharan, P., Agrawal, A., Anjana, R.M., Bhansali, A., Bhardwaj, D., Burkart, K., Cercy, K., Chakma, J.K., Chowdhury, S., Christopher, D.J., Dutta, E., Furtado, M., Ghosh, S., Ghoshal, A.G., Glenn, S.D., Guleria, R., Gupta, R., Jeemon, P., Kant, R., Kant, S., Kaur, T., Koul, P.A., Krish, V., Krishna, B., Larson, S.L., Madhipatla, K., Mahesh, P.A., Mohan, V., Mukhopadhyay, S., Mutreja, P., Naik, N., Nair, S., Nguyen, G., Odell, C. M., Pandian, J.D., Prabhakaran, D., Prabhakaran, P., Roy, A., Salvi, S., Sambandam, S., Saraf, D., Sharma, M., Shrivastava, A., Singh, V., Tandon, N., Thomas, N.J., Torre, A., Xavier, D., Yadav, G., Singh, S., Shekhar, C., Vos, T., Dandona, R., Reddy, K.S., Lim, S.S., Murray, C.J.L., Venkatesh, S., Dandona, L., 2019. The impact of air pollution on deaths, disease burden, and life expectancy across the states of India: the Global Burden of Disease Study 2017. Lancet Planet. Heal. 3, e26–e39. https://doi.org/10.1016/S2542-5196(18)30261-4.

Behera, S.N., Sharma, M., 2011. GIS-based emission inventory , dispersion modeling , and assessment for source contributions of particulate matter in an urban environment, 423–436. https://doi.org/10.1007/s11270-010-0656-x.

Bran, S.H., Srivastava, R., 2017. Investigation of PM2.5mass concentration over India using a regional climate model. Environ. Pollut. 224, 484–493. https://doi.org/10.1016/j.envpol.2017.02.030.

Chafe, Z.A., Brauer, M., Klimont, Z., Van Dingenen, R., Mehta, S., Rao, S., Riahi, K., Dentener, F., Smith, K.R., 2015. Household cooking with solid fuels contributes to ambient $PM_{2.5}$air pollution and the burden of disease. Environ. Health Perspect. 122, 1314–1320. https://doi.org/10.1289/ehp.1206340.

Chin, M., Ginoux, P., Kinne, S., Torres, O., Holben, B.N., Duncan, B.N., Martin, R.V., Logan, J.a., Higurashi, A., Nakajima, T., 2002. Tropospheric aerosol optical thickness from the GOCART model and comparisons with satellite and sun photometer measurements. J. Atmos. Sci. 59, 461–483. https://doi.org/10.1175/1520-0469(2002)059<0461:TAOTFT>2.0.CO;2.

Chowdhury, S., Dey, S., 2016. Cause-specific premature death from ambient PM2.5 exposure in India: estimate adjusted for baseline mortality. Environ. Int. 91, 283–290. https://doi.org/10.1016/j.envint.2016.03.004.

Chowdhury, S., Dey, S., Ghosh, S., Saud, T., 2016. Satellite-Based Estimates of Aerosol Washout and Recovery over India during Monsoon 1302–1314. https://doi.org/10.4209/aaqr.2015.01.0018.

Chowdhury, S., Chafe, Z.A., Pillarisetti, A., Lelieveld, J., 2019. The Contribution of Household Fuels to Ambient Air Pollution in India A Comparison of Recent Estimates Reviewed by.

Chowdhury, S., Dey, S., Girolamo, L. Di, Smith, K.R., Pillarisetti, A., Lyapustin, A., 2019. Tracking ambient PM2.5 build-up in Delhi national capital region during the dry season over 15 years using a high-resolution (1 km) satellite aerosol dataset. Atmos. Environ. 204, 142–150. https://doi.org/10.1016/j.atmosenv.2019.02.029.

Conibear, L., Butt, E.W., Knote, C., Arnold, S.R., Spracklen, D.V., 2018. Residential energy use emissions dominate health impacts from exposure to ambient particulate matter in India. Nat. Commun. 9, 1–9. https://doi.org/10.1038/s41467-018-02986-7.

Dandona, L., Dandona, R., Kumar, G.A., Shukla, D.K., Paul, V.K., Balakrishnan, K., Prabhakaran, D., Tandon, N., Salvi, S., Dash, A.P., Nandakumar, A., Patel, V., Agarwal, S.K., Gupta, P.C., Dhaliwal, R.S., Mathur, P., Laxmaiah, A., Dhillon, P.K., Dey, S., Mathur, M.R., Afshin, A., Fitzmaurice, C., Gakidou, E., Gething, P., Hay, S.I., Kassebaum, N.J., Kyu, H., Lim, S.S., Naghavi, M., Roth, G.A., Stanaway, J.D., Whiteford, H., Chadha, V.K., Khaparde, S.D., Rao, R., Rade, K., Dewan, P., Furtado, M., Dutta, E., Varghese, C.M., Mehrotra, R., Jambulingam, P., Kaur, T., Sharma, M., Singh, S., Arora, R., Rasaily, R., Anjana, R.M., Mohan, V., Agrawal, A., Chopra, A., Mathew, A.J., Bhardwaj, D., Muraleedharan, P., Mutreja, P., Bienhoff, K., Glenn, S., Abdulkader, R.S., Aggarwal, A.N., Aggarwal, R., Albert, S., Ambekar, A., Arora, M., Bachani, D., Bavdekar, A., Beig, G., Bhansali, A., Bhargava, A., Bhatia, E., Camara, B., Christopher, D.J., Das, S.K., Dave, P.V., Dey, S., Ghoshal, A.G., Gopalakrishnan, N., Guleria, R., Gupta, R., Gupta, S.S., Gupta, T., Gupte, M.D., Gururaj, G., Harikrishnan, S., Iyer, V., Jain, S.K., Jeemon, P., Joshua, V., Kant, R., Kar, A., Kataki, A.C., Katoch, K., Khera, A., Kinra, S., Koul, P.A., Krishnan, A., Kumar, A., Kumar, R.K., Kumar, R., Kurpad, A., Ladusingh, L., Lodha, R., Mahesh, P. A., Malhotra, R., Mathai, M., Mavalankar, D., Mohan BV, M., Mukhopadhyay, S., Murhekar, M., Murthy, G.V.S., Nair, S., Nair, S.A., Nanda, L., Nongmaithem, R.S., Oommen, A.M., Pandian, J.D., Pandya, S., Parameswaran, S., Pati, S., Prasad, K., Prasad, N., Purwar, M., Rahim, A., Raju, S., Ramji, S., Rangaswamy, T., Rath, G.K., Roy, A., Sabde, Y., Sachdeva, K.S., Sadhu, H., Sagar, R., Sankar, M.J., Sharma, R., Shet, A., Shirude, S., Shukla, R., Shukla, S.R., Singh, G., Singh, N.P., Singh, V., Sinha, A., Sinha, D.N., Srivastava, R.K., Srividya, A., Suri, V., Swaminathan, R., Sylaja, P.N., Tandale, B., Thakur, J.S., Thankappan, K.R., Thomas, N., Tripathy, S., Varghese, M., Varughese, S., Venkatesh, S., Venugopal, K., Vijayakumar, L., Xavier, D., Yajnik, C.S., Zachariah, G., Zodpey, S., Rao, J.V.R.P., Vos, T., Reddy, K.S., Murray, C.J.L., Swaminathan, S., 2017. Nations within a nation: variations in epidemiological transition across the states of India, 1990–2016 in the Global Burden of Disease Study. Lancet 6736, 1–24. https://doi.org/10.1016/S0140-6736(17)32804-0.

Dey, S., Di Girolamo, L., 2011. A decade of change in aerosol properties over the Indian subcontinent. Geophys. Res. Lett. 38, 1–5. https://doi.org/10.1029/2011GL048153.

Dey, S., Di Girolamo, L., van Donkelaar, A., Tripathi, S.N., Gupta, T., Mohan, M., 2012. Variability of outdoor fine particulate (PM 2.5) concentration in the Indian Subcontinent: a remote sensing approach. Remote Sens. Environ. 127, 153–161. https://doi.org/10.1016/j.rse.2012.08.021.

Dholakia, H.H., Bhadra, D., Garg, A., 2014. Short term association between ambient air pollution and mortality and modification by temperature in five Indian cities. Atmos. Environ. 99, 168–174. https://doi.org/10.1016/j.atmosenv.2014.09.071.

Dudhia, J., 1989. Numerical study of convection observed during the winter monsoon experiment using a mesoscale two-dimensional model. J. Atmos. Sci. https://doi.org/10.1175/1520-0469(1989)046<3077:NSOCOD>2.0.CO;2.

Fast, J.D., Gustafson, W.I., Easter, R.C., Zaveri, R.A., Barnard, J.C., Chapman, E.G., Grell, G.A., Peckham, S.E., 2006. Evolution of ozone, particulates, and aerosol direct radiative forcing in the vicinity of Houston using a fully coupled meteorology-chemistry-aerosol model. J. Geophys. Res. Atmos. 111, 1–29. https://doi.org/10.1029/2005JD006721.

Global Burden of Disease from Major Air Pollution Sources Working Group (GBD-MAPS), 2018, Burden of Disease Attributable to Major Air Pollution Sources in India Special Report.

Grell, G.A., Freitas, S.R., 2014. A scale and aerosol aware stochastic convective parameterization for weather and air quality modeling. Atmos. Chem. Phys. 14, 5233–5250. https://doi.org/10.5194/acp-14-5233-2014.

Grell, G.A., Peckham, S.E., Schmitz, R., McKeen, S.A., Frost, G., Skamarock, W.C., Eder, B., 2005. Fully coupled "online" chemistry within the WRF model. Atmos. Environ. 39, 6957–6975. https://doi.org/10.1016/j.atmosenv.2005.04.027.

Guttikunda, S.K., Calori, G., 2013. A GIS Based Emissions Inventory at 1 Km Â 1 Km Spatial Resolution for Air Pollution Analysis in Delhi , India, p. 67.

Hong, S.-Y., Noh, Y., Dudhia, J., 2006. A new vertical diffusion package with an explicit treatment of entrainment processes. Mon. Weather Rev. 134, 2318–2341. https://doi.org/10.1175/MWR3199.1.

Janssens-Maenhout, G., Dentener, F., Aardenne, J. Van, Monni, S., Pagliari, V., Orlandini, L., Klimont, Z., Kurokawa, J., Akimoto, H., Ohara, T., Wankmüller, R., Battye, B., Grano, D., Zuber, A., Keating, T., 2012. EDGAR-HTAP: a harmonized gridded air pollution emission dataset based on national inventories. JRC Sci. Tech. Rep. https://doi.org/10.2788/14102.

Janssens-Maenhout, G., Crippa, M., Guizzardi, D., Dentener, F., Muntean, M., Pouliot, G., Keating, T., Zhang, Q., Kurokawa, J., Wankmüller, R., Denier Van Der Gon, H., Kuenen, J.J.P., Klimont, Z., Frost, G., Darras, S., Koffi, B., Li, M., 2015. HTAP-v2.2: a mosaic of regional and global emission grid maps for 2008 and 2010 to study hemispheric transport of air pollution. Atmos. Chem. Phys. 15 https://doi.org/10.5194/acp-15-11411-2015.

Joshi, H., Naja, M., Singh, K.P., Kumar, R., Bhardwaj, P., Babu, S.S., Satheesh, S.K., Moorthy, K.K., Chandola, H.C., 2016. Investigations of aerosol black carbon from a semi-urban site in the Indo-Gangetic Plain region. Atmos. Environ. 125, 346–359. https://doi.org/10.1016/j.atmosenv.2015.04.007.

Klimont, Z., Kupiainen, K., Heyes, C., Purohit, P., Cofala, J., Rafaj, P., Borken-Kleefeld, J., Schöpp, W., 2017. Global anthropogenic emissions of particulate matter including black carbon. Atmos. Chem. Phys. 17, 8681–8723. https://doi.org/10.5194/acp-17-8681-2017.

Kompalli, S.K., Babu, S.S., Moorthy, K.K., Manoj, M.R., Kumar, N.V.P.K., Shaeb, K.H.B., Joshi, A.K., 2014. Aerosol black carbon characteristics over Central India: Temporal variation and its dependence on mixed layer height. Atmos. Res. 147–148, 27–37. https://doi.org/10.1016/j.atmosres.2014.04.015.

Kumar, R., Nagar, J.K., Kumar, H., Kushwah, A.S., Meena, M., Kumar, P., Raj, N., Singhal, M.K., Gaur, S.N., 2007. Association of indoor and outdoor air pollutant level with respiratory problems among children in an industrial area of Delhi, India. Arch. Environ. Occup. Health 62, 75–80. https://doi.org/10.3200/AEOH.62.2.75-80.

Li, M., Zhang, Q., Kurokawa, J.I., Woo, J.H., He, K., Lu, Z., Ohara, T., Song, Y., Streets, D. G., Carmichael, G.R., Cheng, Y., Hong, C., Huo, H., Jiang, X., Kang, S., Liu, F., Su, H., Zheng, B., 2017. MIX: a mosaic Asian anthropogenic emission inventory under the international collaboration framework of the MICS-Asia and HTAP. Atmos. Chem. Phys. 17, 935–963. https://doi.org/10.5194/acp-17-935-2017.

Lin, Y.-L., Farley, R.D., Orville, H.D., 1983. Bulk parameterization of the snow field in a cloud model. J. Clim. Appl. Meteorol. https://doi.org/10.1175/1520-0450(1983)022<1065:BPOTSF>2.0.CO;2.

Martin, R.V., Brauer, M., Donkelaar, A. Van, Shaddick, G., Narain, U., Dey, S., 2019. Atmospheric Environment : X No one knows which city has the highest concentration of fi ne particulate matter. Atmos. Environ. X 3, 100040. https://doi.org/10.1016/j.aeaoa.2019.100040.

Mlawer, E.J., Taubman, S.J., Brown, P.D., Iacono, M.J., Clough, S.A., 1997. Radiative transfer for inhomogeneous atmospheres: RRTM, a validated correlated-k model for the longwave. J. Geophys. Res. Atmos. 102, 16663–16682. https://doi.org/10.1029/97JD00237.

Modeling, G., Office, A., Systems, S., Applications, S., Corporation, I., 2017. The Modern-Era Retrospective Analysis for Research and Applications, vol. 2, pp. 5419–5454. https://doi.org/10.1175/JCLI-D-16-0758.1.

OECD, 2016. The Economic Consequences of Outdoor Air Pollution. https://doi.org/10.1787/9789264257474-en.

Pachauri, T., Singla, V., Satsangi, A., Lakhani, A., Kumari, K.M., 2013. Characterization of carbonaceous aerosols with special reference to episodic events at Agra, India. Atmos. Res. 128, 98–110. https://doi.org/10.1016/j.atmosres.2013.03.010.

Pande, J.N., Bhatta, N., Biswas, D., Pandey, R.M., Ahluwalia, G., Siddaramaiah, N.H., Khilnani, G.C., 2002. Outdoor air pollution and emergency room visits at a hospital in Delhi. Indian J. Chest Dis. Allied Sci. 44, 13–19.

Pandey, a., Sadavarte, P., Rao, A.V., Venkataraman, C., 2014. A technology-linked multi-pollutant inventory of Indian energy-use emissions: II. Residential, agricultural and informal industry sectors. Atmos. Environ. 99, 341–352. https://doi.org/10.1016/j.atmosenv.2014.09.080.

Rajarathnam, U., Sehgal, M., Nairy, S., Patnayak, R.C., Chhabra, S.K., Kilnani, Ragavan, K.V.S., 2011. Part 2. Time-series study on air pollution and mortality in Delhi. Res. Rep. Health Eff. Inst. 47–74.

Ram, K., Sarin, M.M., 2010. Spatio-temporal variability in atmospheric abundances of EC, OC and WSOC over Northern India. J. Aerosol Sci. 41, 88–98. https://doi.org/10.1016/j.jaerosci.2009.11.004.

Rao, S.T., Galmarini, S., Puckett, K., 2010. Air quality model evaluation international initiative (AQMEII): advancing the state of the science in regional photochemical modeling and its applications. Bull. Am. Meteorol. Soc. 92, 23–30. https://doi.org/10.1175/2010BAMS3069.1.

Sadavarte, P., Venkataraman, C., 2014. Trends in multi-pollutant emissions from a technology-linked inventory for India: I. Industry and transport sectors. Atmos. Environ. 99, 353–364. https://doi.org/10.1016/j.atmosenv.2014.09.081.

Sagar, A., Balakrishnan, K., Guttikunda, S., Roychowdhury, A., Smith, K.R., 2016. India leads the way: a health-centered strategy for air pollution. Environ. Health Perspect. 124, A116–A117. https://doi.org/10.1289/EHP90.

Sharma, M., Dixit, O., 2016. Comprehensive Study on Air Pollution and Green House Gases (GHGs) in Delhi. DPCC.

Stockwell, W.R., Middleton, P., Chang, J.S., Tang, X., 1990. The second generation regional acid deposition model chemical mechanism for regional air quality modeling. J. Geophys. Res. Atmos. 95, 16343–16367. https://doi.org/10.1029/JD095iD10p16343.

Stohl, A., Aamaas, B., Amann, M., Baker, L.H., Bellouin, N., Berntsen, T.K., Boucher, O., Cherian, R., Collins, W., Daskalakis, N., Dusinska, M., Eckhardt, S., Fuglestvedt, J.S., Harju, M., Heyes, C., Hodnebrog, Hao J., Im, U., Kanakidou, M., Klimont, Z., Kupiainen, K., Law, K.S., Lund, M.T., Maas, R., MacIntosh, C.R., Myhre, G., Myriokefalitakis, S., Olivié, D., Quaas, J., Quennehen, B., Raut, J.C., Rumbold, S.T., Samset, B.H., Schulz, M., Seland, Shine, K.P., Skeie, R.B., Wang, S., Yttri, K.E., Zhu, T., 2015. Evaluating the climate and air quality impacts of short-lived pollutants. Atmos. Chem. Phys. 15, 10529–10566. https://doi.org/10.5194/acp-15-10529-2015.

Tewari, M., Wang, W., Dudhia, J., LeMone, M.A., Mitchell, K., Ek, M., Gayno, G., Wegiel, J., Cuenca, R.H., 2014. Clay n.d.

Upadhyay, A., Dey, S., Chowdhury, S., Goyal, P., 2018. Expected health bene fi ts from mitigation of emissions from major anthropogenic PM 2 . 5 sources in India : statistics at state level *. Environ. Pollut. 242, 1817–1826. https://doi.org/10.1016/j.envpol.2018.07.085.

Upadhyay, A., Dey, S., Goyal, P., Dash, S.K., 2018. Projection of near-future anthropogenic PM 2 . 5 over India using statistical approach. Atmos. Environ. 186, 178–188. https://doi.org/10.1016/j.atmosenv.2018.05.025.

van Donkelaar, A., Martin, R.V., Brauer, M., Kahn, R., Levy, R., Verduzco, C., Villeneuve, P.J., 2010. Global estimates of ambient fine particulate matter concentrations from satellite-based aerosol optical depth: development and application. Environ. Health Perspect. 118, 847–855. https://doi.org/10.1289/ehp.0901623.

Van Donkelaar, A., Martin, R.V., Brauer, M., Hsu, N.C., Kahn, R.A., Levy, R.C., Lyapustin, A., Sayer, A.M., Winker, D.M., 2016. Global estimates of fine particulate matter using a combined geophysical-statistical method with information from satellites, models, and monitors. Environ. Sci. Technol. 50, 3762–3772. https://doi.org/10.1021/acs.est.5b05833.